Synthesis and in vitro testing of thermoresponsive polymer-grafted core-shell magnetic mesoporous silica nanoparticles for efficient controlled and targeted drug delivery

UNIVERSITÀ DEGLI STUDI DI TORINO

Synthesis and in vitro testing of thermoresponsive polymer-grafted core-shell magnetic mesoporous silica nanoparticles for efficient controlled and targeted drug delivery

Marcos E. Peralta[a], Sushilkumar A. Jadhav[b,c,*], Giuliana Magnacca[b], Dominique Scalarone[b], Daniel O. Mártire[d], María E. Parolo[e], Luciano Carlos[a,*]

[a] Instituto de Investigación y Desarrollo en Ingeniería de Procesos, Biotecnología y Energías Alternativas, PROBIEN (CONICET-UNCo), Facultad de Ingeniería, Universidad Nacional Del Comahue, Buenos Aires 1400, 8300 Neuquén, Argentina.

[b] University of Torino, Department of Chemistry and NIS Research Centre, Via P. Giuria 7, 10125 Torino, Italy.

[c] School of Nanoscience and Technology, Shivaji University Kolhapur, 416004 Kolhapur, Maharashtra, India

[d] Instituto de Investigaciones Fisicoquímicas Teóricas y Aplicadas (INIFTA), CCT-La Plata-CONICET, Universidad Nacional de La Plata, 1900 La Plata, Argentina.

[e] Centro de Investigaciones en Toxicología Ambiental y Agrobiotecnología del Comahue, CITAAC (CONICET-UNCo), Facultad de Ingeniería, Universidad Nacional Del Comahue, Buenos Aires 1400, 8300 Neuquén, Argentina.

* Corresponding author. E-mail address: sushil.unige@gmail.com (S.A.J.), luciano.carlos@probien.gob.ar (L.C.); Tel: (+91)2312609490 (S.J.), (+54)2994490300 (L.C.).

Abstract

In this work, thermoresponsive polymer grafted magnetic mesoporous silica nanoparticles were prepared, fully characterized and tested as controlled drug delivery systems. For this purpose, iron oxide nanoparticles coated with mesoporous silica shell were grafted with poly(N-isopropylacrylamide-co-3-(methacryloxypropyl)trimethoxysilane) (PNIPAM-co-MPS). The grafting and polymerization on the as-prepared nanoparticles were performed in one-step procedure. Using this methodology, the polymer was successfully grafted mainly onto the silica surface, leaving the mesopores empty for the drug loading. The prepared hybrid nanoparticles (MMSNP-PNIPAM-co-MPS) showed high magnetization saturation (19.5 emu g^{-1}) and high specific surface area (505 m^2 g^{-1}) and pore volume (0.29 cm^3 g^{-1}). Ibuprofen was used as a model drug to test the performance of the hybrid particles as thermosensitive drug delivery systems. For this, *in vitro* drug delivery tests were conducted below (25°C) and above (40°C) the lower critical solution temperature (LCST) of the polymer (PNIPAM-co-MPS). Considerable difference (80%) in the ibuprofen release at these two temperatures was observed and a fast and complete release of the drug at 40°C was observed. These results suggest that the thermoresponsive copolymer acts as a gatekeeper for the temperature-controlled release of the drug loaded inside the mesopores. Therefore, MMSNP-PNIPAM-co-MPS are promising magnetic and thermoresponsive nanocarriers for targeted delivery of therapeutic substances.

Keywords: Drug delivery, magnetic nanoparticles, mesoporous silica nanoparticles, temperature-controlled release, thermoresponsive polymer

1. Introduction

In recent decades, nanotechnology has been widely used to develop new diagnostic and therapeutic strategies for the treatment of various diseases. In this sense, the development of drug nanocarriers that deliver the therapeutic substances at target organs in the body, control the kinetic release and protect drugs from being metabolized or excreted prematurely from the body has become an important issue [1–3]. A wide variety of nanomaterials have been designed for this purpose, including liposomes, polymer nanoparticles, micelles, dendrimers, inorganic nanoparticles, quantum dots, and metal oxide frameworks [2]. Since their first application as drug delivery systems [4], mesoporous silica nanoparticles (MSNPs) have been widely studied for various biomedical applications due to their outstanding properties, such as controllable particle size and morphology, high specific surface area and pore volume, low toxicity, hemocompatibility, and ease of surface modification [5–7]. The ability to control precisely the drug release can be achieved by modifying the MSNPs surface with appropriate release triggers that specifically react with response to stimuli, which can be either endogenous (pH [8,9], chemical agents [10,11], and redox gradients [12,13]) or exogenous (temperature [14,15], magnetic field [16], ultrasound intensity [17], and light [18]).

Thermoresponsive polymers undergo a *coil-to-globule* transition when the temperature is changed. This transition happens at the lower critical solution temperature (LCST) of the polymer [19]. Poly(*N*-isopropylacrylamide) (PNIPAM) is among the most investigated thermoresponsive polymers [20], which has its LCST around 30-32°C, interesting for drug delivery applications [21]. PNIPAM contains a hydrophobic as well as a hydrophilic moiety. The isopropylic moiety is hydrophobic whereas the amide moiety is hydrophilic. Below the LCST, the thermoresponsive polymer exhibits a hydrophilic nature and the polymer chains are present in extended hydrated “coil” conformation. In contrast, above the LCST, polymer chains become hydrophobic and collapse in a compressed “globule” conformation. For most drug delivery applications, pure PNIPAM is not suitable since the body temperature is higher than their LCST. Thus, the LCST of PNIPAM is commonly adjusted by the addition of salts, surfactants or by performing a copolymerization with hydrophilic or hydrophobic co-monomers [22]. In particular, the hydrophobic monomers decrease the LCST while the hydrophilic monomers help to raise the LCST. For instance, reported studies have shown an increased in the LCST of PNIPAM after carrying out its copolymerization with methacrylic acid [23]. Also, the copolymerization of 3-(methacryloxypropyl)trimethoxy silane (MPS) with *N*-isopropylacrylamide (NIPAM) gives an interesting thermoresponsive polymer that can be anchored on silica surface with a LCST of 36°C [24]. This thermo-reversible transition of the polymer can be used to apply an on-off gatekeeper mechanism to porous particles containing guest molecules. For instance, expanded-pore MSNPs co-functionalized with PNIPAM and poly(ethylene glycol) were applied for temperature control release of bovine hemoglobin [25]. Although PNIPAM-based systems were the focus of various studies as drug nanocarriers, many of them showed an undesirable and significant release of the payload below the LCST [26]. For this reason, it is important to improve the gatekeeper performance of these systems for medical application.

Magnetic-responsive nanomaterials are used in biomedical applications such as targeted drug delivery and hyperthermia [27,28]. They are also used in magnetic resonance imaging and to integrate diagnostics and therapy in a single system [29–32]. In this context, magnetic mesoporous silica-based nanoparticles (MMSNPs) can be used as a magnetic targeted drug delivery systems. Hegazy and co-workers [33] prepared core-shell MMSNP with a magnetite core and a mesoporous silica shell functionalized with PNIPAM copolymer with disulfide bonds in a multi-step procedure and tested for the controlled release of doxorubicin (DOX). On the

other hand, a thermoresponsive copolymer of NIPAM and methacrylic acid was grafted by two step procedure on MMSPN by Tian et al. [34] and was used as an on-off drugs release system.

This work reports the preparation of magnetic and temperature-responsive drug nanocarriers based on thermoresponsive polymer (PNIPAM-co-MPS)-grafted magnetic mesoporous silica core-shell nanoparticles (MMSNP-PNIPAM-co-MPS). The synthesis approach consisted the one-step grafting and polymerization of the polymer on silica surface. The thermosensitive behaviour of the copolymer was used to make it act as a gatekeeper for the release of the drug loaded inside the pores. Ibuprofen, a well-known anti-inflammatory drug was used to test the performance of the hybrid drug delivery systems. An efficient temperature controlled on-off release and high magnetic saturation were observed in MMSNP-PNIPAM-co-MPS. The results indicate that MMSNP-PNIPAM-co-MPS are promising candidates as advanced targeted and stimuli responsive drug delivery systems.

2. Materials and Methods

2.1 Materials

Iron (III) chloride hexahydrate ($FeCl_3.6H_2O$, purity > 99%) was purchased by Merck, ethylene glycol by Riedel-de Haën and sodium acetate trihydrate (purity > 99%) by Fluka Chemika. Tetraethoxylsilane (TEOS), ammonium hydroxide (30%), cetyltrimethylammonium bromide (CTAB), N-isopropylacrylamide (NIPAM), 3-(methacryloxypropyl)trimethoxy silane (MPS), azobisisobutyronitrile (AIBN) and ibuprofen (IBU) were purchased from Sigma-Aldrich. All aqueous solutions were prepared using water of Milli-Q grade (Millipore).

2.2. Synthesis of magnetic mesoporous silica nanoparticles (MMSNP)

Magnetic Iron oxide nanoparticles (NPs) were prepared by solvothermal method [35]. Briefly, 1.35 g of $FeCl_3.6H_2O$ and 6.0 g of sodium acetate trihydrate were dissolved in 50 mL of ethylene glycol on a Teflon container. Later, the Teflon container was put on a stainless-steel autoclave reactor and heated at 200°C for 8 h. The obtained precipitate was magnetically separated by using neodymium magnet and washed with ethanol. This washing step was repeated with distilled water three times. In all the washing steps, the solid were separated from the supernatant using magnetic separation. Then, the iron oxide nanoparticles (NPs) were coated with a first thin non-porous silica layer through the following procedure: 500 mg of magnetite were dispersed by ultrasound in a glass flask containing 125 mL of an ethanol/water 4:1 solution. Later, 1.25 mL of concentrated ammonia solution was added followed by drop wise addition of 1 mL TEOS. The mixture was stirred at 65°C for 5 h. The obtained grey solid was magnetically separated and washed with the solvent solution (i.e. ethanol/water 4:1) three times. Later, a mesoporous silica coating onto the magnetic NPs was performed according to reported procedures [36,37]. Briefly, the as-prepared non-porous silica coated magnetite NPs, 500 mg of CTAB and 1.75 mL of ammonia solution were mixed in 250 mL of water. The suspension was kept under vigorous stirring and heating up to 80°C. When the temperature reached 80°C, 2.5 mL of TEOS was added dropwise and the sol-gel reaction was kept at 80°C for 2 h. After cooling at room temperature, the solid obtained was magnetically separated, washed three times with distilled water and dried in an oven at 70°C overnight. Finally, the obtained solid was calcinated in a tubular oven (Carbolite) applying a ramp of 2 °C min^{-1} up to 500°C in nitrogen atmosphere and then the temperature was kept at 500°C in air flow for 2 h. This product was named MMSNP.

2.3. Synthesis of thermoresponsive polymer coated magnetic mesoporous silica nanoparticles (MMSNP-PNIPAM-co-MPS)

The thermoresponsive polymer grafting on MMSNP was carried out by a one-step synthesis procedure [24,38]. 500 mg of MMSNP were placed in a two neck round bottom flask with 125 mg of NIPAM and 18 mL of dry ethanol. The flask was connected to a condenser fitted with a nitrogen balloon and the suspension was stirred under nitrogen atmosphere. Thereafter, 13 µL of MPS and 2 mL of AIBN ethanol solution (0.3 wt. %) were added in sequence and the reaction mixture was heated for 16 h at 70°C. During this step, a simultaneous radical polymerization between the co-monomers and grafting with the silica surface of MMSNP occurs. At the end of the reaction, the nanoparticles were washed three times with ethanol, magnetically separated and dried overnight at 70°C. These nanoparticles were named as MMSNP-PNIPAM-co-MPS. A complete scheme of the synthesis steps for obtaining MMSNP-PNIPAM-co-MPS is shown in Fig. 1.

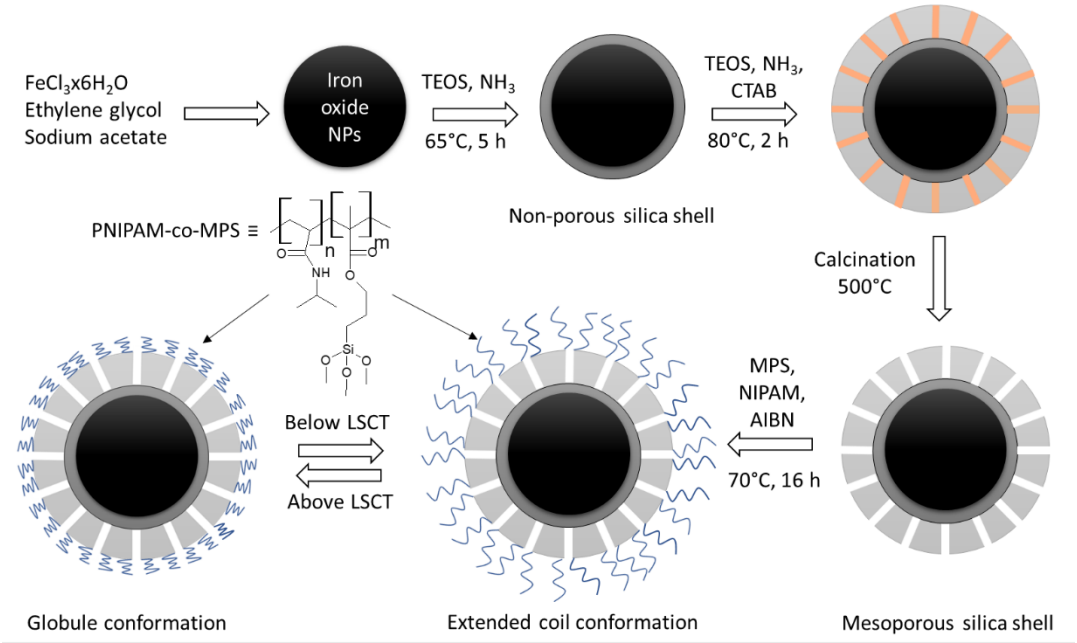

Fig. 1. Synthesis procedure of MMSNP-PNIPAM-co-MPS nanoparticles.

2.4. Characterization techniques

ATR-Fourier transform infrared (FTIR) spectra were measured by using a Spectrum 100 instrument (PerkinElemer) in the attenuated total reflectance (ATR) mode with a diamond crystal in the range 600 – 4000 cm^{-1}. X-ray diffraction (XRD) patterns were performed on a X'Pert PRO MPD diffractometer from PANalytical equipped with Cu anode (45 kV, 40 mA). The XRD patterns were recorded in the range of 2θ value between 20° and 70°. Data management was performed using X'Pert HighScore software. N_2 adsorption–desorption isotherms at 77K were obtained using a gas adsorption apparatus (ASAP 2020, Micromeritics). Specific surface areas (SSA) were calculated using the Brunauer–Emmett–Teller (BET) model. Pore size distribution and pore volume were calculated on the adsorption branch of the isotherms according to the Barrett–Joyner–Halenda (BJH) method. Thermogravimetric analyses (TGA) were performed with a Q500 Thermogravimetric Analyzer (TA Instruments). The samples were pre-dried for a short time of 30 min at 100°C before the analysis. The analysis were carried out by heating samples at a rate of 10°C min^{-1} from room temperature to 600°C in a nitrogen atmosphere and from 600 to 700°C in air. Transmission electron microscopy (TEM) images

were recorded with a JEOL 2010 instrument equipped with a LaB_6 filament and acceleration voltage of 300 kV. Samples were deposited onto holed carbon-coated copper grids by dry deposition. A Malvern Zetasizer Nano ZS90 instrument (Malvern) was employed in the Dynamic Light Scattering (DLS) measurements. Nanoparticles dispersion in milli Q water (0.1%) were sonicated for 20 min before the DLS analysis. Magnetic properties were recorded by using a LakeShore 7300 vibrating sample magnetometer. Magnetization curves were registered at 300 K with a magnetic field cycled between −10,000 and 10,000 G.

2.5. Ibuprofen loading and release tests

For the drug loading, nanoparticles were dispersed in a flask with a hexane solution of ibuprofen (0.16 M), then the dispersion was put in a chamber at 40°C and kept under stirring for 24 h. Later, the nanoparticles were magnetically separated, washed with hexane and distilled water and dried at room temperature. Ibuprofen loading was estimated by TGA and UV-visible spectroscopy. The loading from TGA was calculated by subtracting the amount of polymer, adsorbed water and the loss derived from dehydroxylation process from the total weight loss of the loaded nanoparticles. For UV-visible spectroscopy, the loading was estimated from the total amount of ibuprofen released from a dispersion of the loaded nanoparticles in physiological saline solution (PSS) at 40 °C in 24 h. UV–Vis analyses were performed using a T60 UV–Vis spectrophotometer (PG instruments). Ibuprofen quantification was performed measuring Abs values at λ = 264 nm (ε_{264nm} = 346.2 cm^{-1} M^{-1}, this value was obtained from the calibration curve, data not shown).

The *in vitro* drug release tests were carried out in PSS solution. A proper amount (10 – 15 mg) of ibuprofen loaded nanoparticles were dispersed in a flask containing 40 mL of PSS solution. At defined time intervals, the nanoparticles were magnetically separated and an aliquot of the supernatant was withdrawn and analysed by UV–vis spectroscopy at 264 nm. The assays were conducted at 25°C (below LCST) and 40°C (above LCST) by triplicate.

3. Results and Discussion

3.1. Characterization

The morphology of the as-synthetized nanoparticles were observed with TEM images. No significant difference can be seen between MMSNP and hybrid MMSNP-PNIPAM-co-MPS (for brevity only of MMSNP-PNIPAM-co-MPS images are shown in Fig. 2A and 2B). The polymer-grafting on MMSNP does not affect the primary structure of the particles. The NPs seem to be quasi-spherical with a crystalline iron oxide core, visible for the higher optical density, and a porous silica shell. The analysis of the fringe patterns in the iron oxide core reveals the presence of the crystalline plane d_{hkl} = 2.7 nm corresponding to the (3 1 0) plane of maghemite (γ-Fe_2O_3) (Fig. 2B). The bare iron oxide NPs (Fig. S1, Supporting information) have a mean diameter of 76 nm (Fig. 2C). A uniform thickness of circa 15 nm of mesoporous silica shell around the particles can be seen. The mean diameter of the MMSNP was 91 nm.

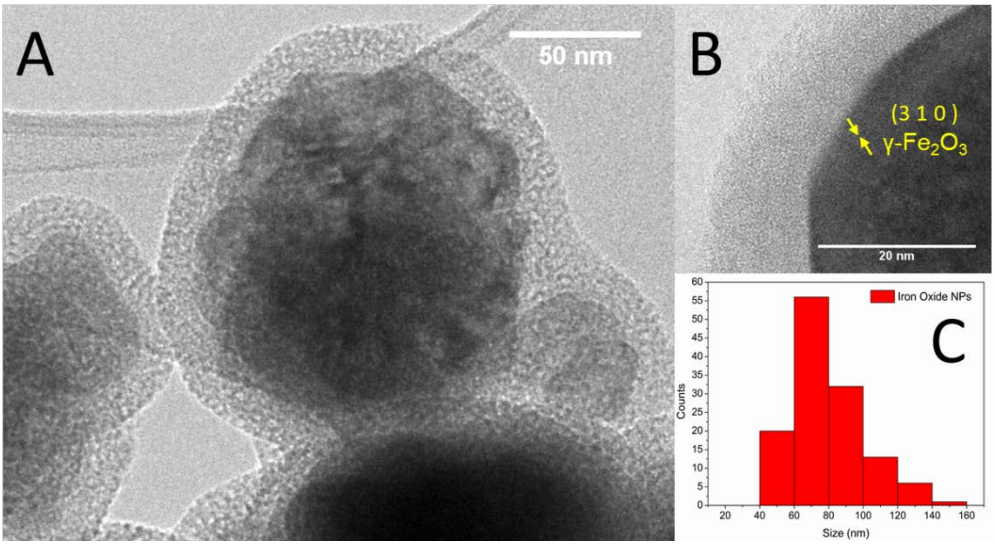

Fig. 2. TEM Images of (A, B) MMSNP-PNIPAM-co-MPS and size distribution of iron oxide NPs (C).

In order to confirm the presence of iron oxide and identify the relative crystalline phases formed, XRD diffraction patterns of iron oxide NPs and MMSNP-PNIPAM-co-MPS (Fig. 3) were recorded. All peak positions at $2\theta = 18.3$, 30.1, 34.4, 37.1, 43.0, 53.4, 56.9 and 62.5° can be associated with (111), (229), (311), (222), (400), (422), (511) and (440) X-ray diffraction planes of cubic magnetite phase (Card number 01-077-1545, ICCD Database). However, the presence of maghemite cannot be discarded since XRD is not a suitable technique to distinguish between both phases because of XRD patterns of magnetite and maghemite are very similar [39]. A broad diffraction halo centred around 2θ = 23.5° in MMSNP-PNIPAM-co-MPS XRD diffraction pattern can be attributed to mesoporous silica [40]. As expected, the grafting and polymerization step did not modify the iron oxide crystallographic features since the diffraction patterns of both samples present the same diffraction peaks associated to iron oxides.

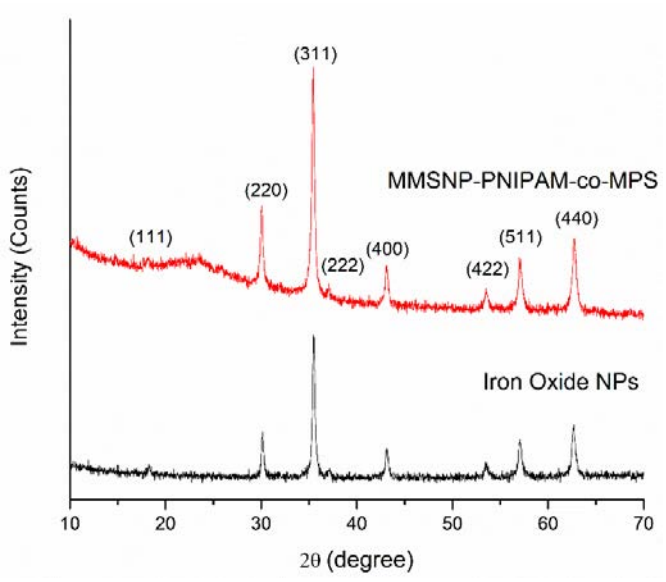

Fig. 3. X-ray diffraction patterns of Iron Oxide NPs (black line) and MMSNP-PNIPAM-co-MPS (red line).

The presence of the porous silica shell and the polymer-grafting on MMSNPs was confirmed by ATR-FTIR analysis. An intense absorption band due to the vibration modes of the silica tetrahedral framework between 1300 and 800 cm^{-1} was observed in MMSNPP and MMSNPP-PNIPAM spectrum (Fig. S2, Supporting Material), confirming what evidenced in HR-TEM images. A sample of neat copolymer of NIPAM and MPS was prepared for comparison purposes by following the procedure described in the section 2.3. The thermoresponsive polymer characteristic bands at 1710 cm^{-1} ($\nu_{C=O}$, methacryloxypropyl of MPS), 1638 cm^{-1} ($\nu_{C=O}$, amide), 1536 cm^{-1} (ν_{C-N}), 1458 cm^{-1} (ν_{C-H}), 1370 cm^{-1} and 1390 cm^{-1} (δ deformation and bending, C-H) [41] were observed in the spectrum of MMSNP-PNIPAM-co-MPS and PNIPAM-co-MPS. (Fig. 4). It is worth mentioning that the higher signal at 1710 cm^{-1} than expected for the neat copolymer PNIPAM-co-MPS indicates that the composition of the free and grafted copolymer might not be exactly the same due to the different reaction environment (i.e. presence of NPs). Possibly, after the polymerization some of the MPS moieties grafted to the silica NPs remain there and do not co-polymerize with NIPAM.

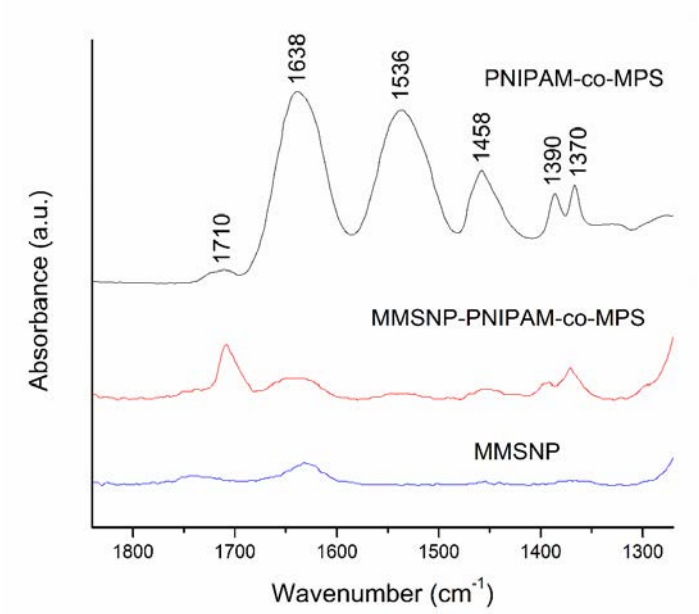

Fig. 4. ATR-IR spectra of MMSNP (blue line), MMSNP-PNIPAM-co-MPS (red line) and PNIPAM-co-MPS polymer reference (black line) samples.

Thermogravimetric analysis was used to quantify the amount of polymer grafted to MMSNP-PNIPAM-co-MPS. The TGA curve of bare nanoparticles (blue solid line, Fig. 5) shows a first weight loss at 100°C, because of water molecules desorption, and a smooth weigh loss from 100 to 700°C, probably related to surface dehydroxylation. In polymer coated nanoparticles (red dashed line, Fig. 5) this second weight loss is increased to about 8.5%, due to thermal decomposition of the organic polymer matter. The total weight loss from MMSNP and MMSNP-PNIPAM-co-MPS was 2.7% and 8.5%, when the samples were heated up to 700°C. Thus, the amount of polymer grafted results to be around 5.8%.

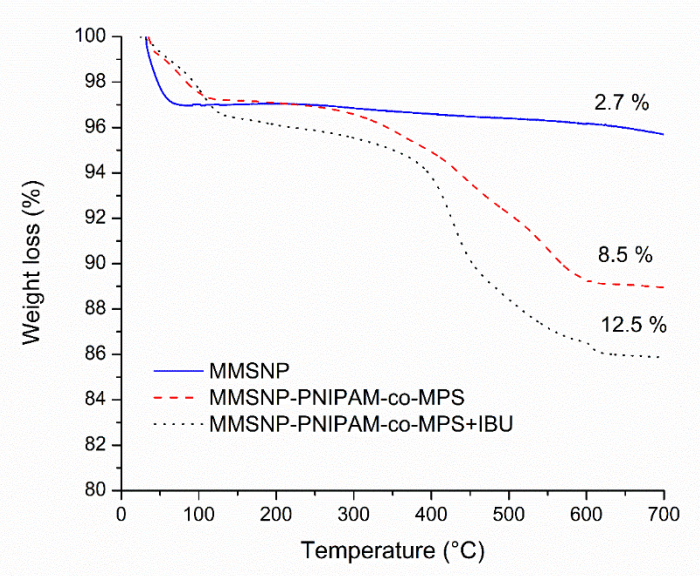

Fig. 5. TGA curves of MMSNP (blue solid line), MMSNP-PNIPAM-co-MPS (red dashed line) and MMSNPP-PNIPAM-co-MPS ibuprofen loaded (MMSNP-PNIPAM-co-MPS + IBU) (black dotted line) samples.

The N_2 adsorption-desorption isotherms (Fig. 6A) at 77 K of MMSNP and MMSNP-PNIPAM are characteristic of mesoporous materials with a type IV isotherm and H1-type hysteresis loop according to IUPAC classification [42]. After grafting of MPS and subsequent polymerization, non-significant differences of area and porosity were observed. The specific surface area was reduced from 521 $m^2\,g^{-1}$ to 505 $m^2\,g^{-1}$, the pore volume from 0.33 $cm^3\,g^{-1}$ to 0.29 cm^3g^{-1} and the mean pore size from 29 Å to 27 Å (fig. 6B). These results can be accounted for the presence of small fraction of polymer chains inside the mesopores and suggest that a PNIPAM-co-MPS layer was mainly grown on top the mesoporous silica surface. Previous results from a two-step grafting and polymerization procedure showed a significant grafting of PNIPAM inside the silica mesopores [15,43]. Thus, the one-step grafting and polymerization approach seems to favour the grafting of the polymer on the external surface of the mesoporous silica particles.

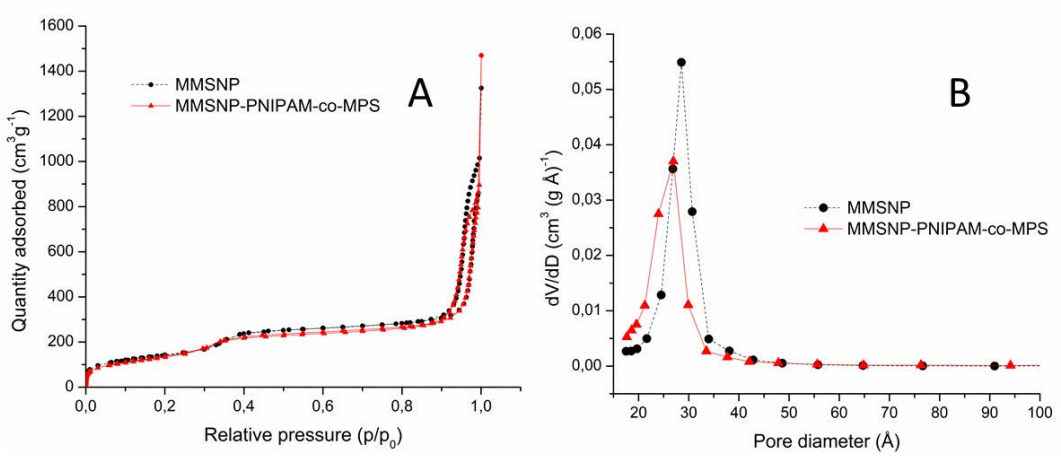

Fig. 6. A) Nitrogen adsorption-desorption isotherms and B) BJH pore size distribution of MMSNP (black circles and dashed line) and MMSNP-PNIPAM-co-MPS (red triangles and solid line).

The thermoresponsive behaviour of the polymer grafted on the surface of the particles was checked by DLS. The results showed that the average hydrodynamic diameter (D_h) of the bare MMSNP was ≈92 nm (Fig. 7A). This diameter did not change with temperature. The narrow distribution with an average D_h value similar to the mean diameter of the nanoparticles found from TEM images (≈91 nm) indicates that the nanoparticles are reasonably monodisperse. Fig. 7B shows the temperature dependence of the D_h of the polymer-grafted MMSNPs. The average D_h decreased from 125 nm at 25°C to 105 nm at 40°C, evidencing the thermoresponsive behaviour of the polymer grafted on the nanoparticles. At temperature below LCST, the polymer chains are in their extended hydrophilic coil form, with their polar groups interacting with water molecules by hydrogen bonds, whereas at temperature above LCST, the hydrophobic polymer segments start to increase their reciprocal interaction changing their configuration to a globular-like hydrophobic form falling on the particles surface. This transition results in reduction of the D_h of the nanoparticles.

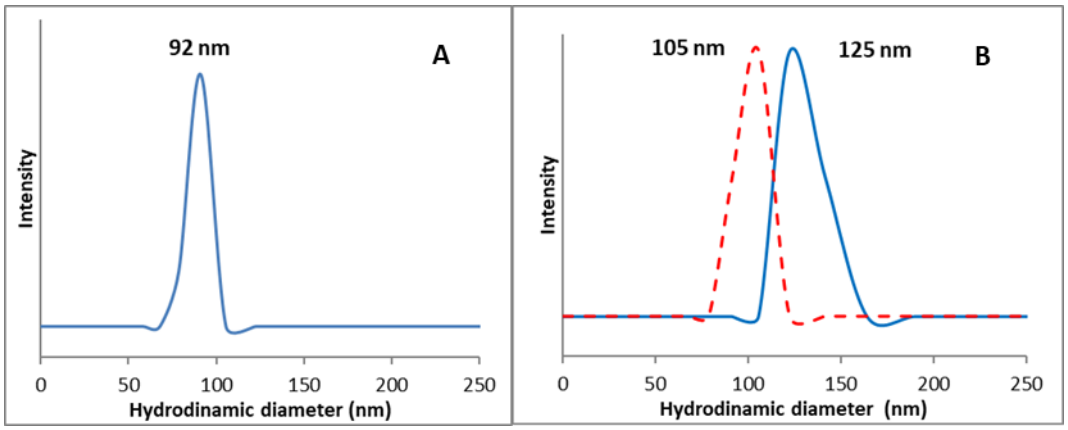

Fig. 7. Particle size distribution of MMSNP (A) and MMSNP-PNIPAM-co-MPS (B) nanoparticles at 20 °C (solid blue line) and at 40 °C (dotted red line) as measured by DLS.

Fig. 8 reports the magnetization curves obtained for iron oxide cores and silica-based nanocarriers. At 300 K, all samples exhibited soft ferromagnetic behaviour with low coercivity and remanence (Table S1 in the supporting material). The magnetic saturation (Ms) for iron oxide core, MMSNP and MMSNP-PNIPAM-co-MPS were 79.5 emu g^{-1}, 26.5 emu g^{-1} and 19.5 emu g^{-1}, respectively. The smaller Ms values observed for the nanocarriers than pure iron oxide nanoparticles can be attributed to silica and subsequent polymer coating [40,44]. Despite the decrease in the Ms value, MMSNP-PNIPAM-co-MPS still present high Ms (19.5 emu g^{-1}) compared with previously reported magnetic nanocarriers based on silica coated iron oxide nanoparticles (Ms ~ 2.1 - 2.6 emu g^{-1}) [33,45], highlighting the potential applicability of MMSNP-PNIPAM-co-MPS as a magnetic-targeted drug nanocarriers.

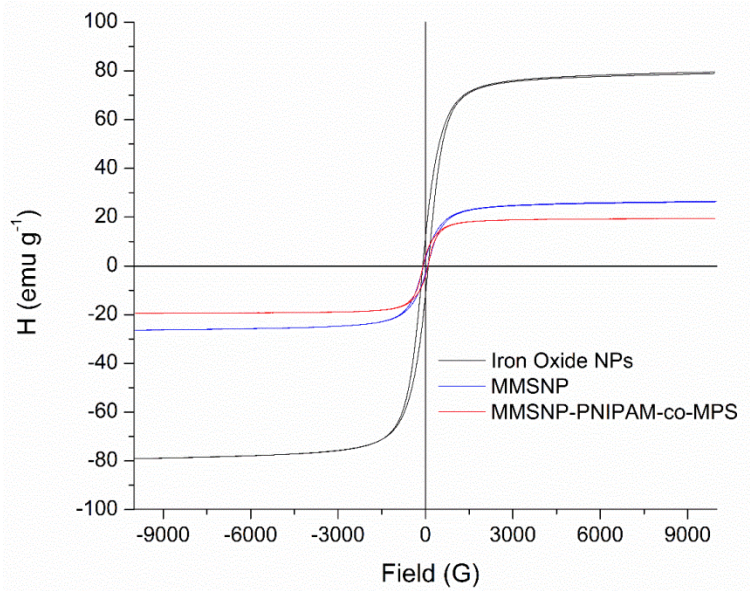

Fig. 8. Magnetization curves of iron oxide NPs, MMSNP and MMSNP-PNIPAM-co-MPS at 300 K.

3.2. Ibuprofen release tests

Ibuprofen was used to test the performance of hybrid MMSNP-PNIPAM-co-MPS as magnetic and temperature-controlled drug delivery system. The drug loading was performed at 40°C in hexane. The quantitative loading of ibuprofen was estimated by UV-vis spectroscopy and TGA. As described in section 2.5 from both analysis similar loading results were obtained. The estimated ibuprofen content was 24.0 wt% from UV-Vis and 21.0 wt% from TGA for MMSNP and 6.2 wt% from UV-Vis and 4.0 wt% from TGA (Fig. 5) for MMSNP-PNIPAM-co-MPS. Although the presence of the polymer did not significantly affect the textural properties of the nanoparticles (i.e. surface area, pore volume, etc.), the lower ibuprofen loading in MMSNP-PNIPAM-co-MPS with respect to the non-functionalized sample, could indicate that the polymer chains at the edge of the mesopores hinder to some extent the diffusion of ibuprofen.

The *in vitro* drug release tests of ibuprofen were performed below (25°C) and above (40°C) the LCST of the thermoresponsive grafted polymer. No temperature effect was observed for the quick release of Ibuprofen from bare MMSNP (Fig. 9A), whereas after PNIPAM-co-MPS grafting the release profiles become temperature dependent (Fig. 9B). Below the LSCT (25°C), the polymer chains are in their fully extended form and they cover the pores, thus hindering the ibuprofen release. Only a 20% release of the payload was observed after 16 h, which is a very good result considering previous studies reporting higher percentages of IBU release at temperatures below LCST for other PNIPAM-based materials [24,46–49]. Above the LSCT (40°C), the polymer undergoes a coil-to-globule transition by contracting in a compact form leaving the pores open, which in turn results in the complete release of the drug in less than 24 h (Fig. 9B). The differences observed in the % of IBU release between both temperatures at 16 h (around 80%) indicate that the synthesized material presents an excellent temperature-controlled release feature. In comparison to other reports that showed an incomplete and slow release of drug from similar PNIPAM-based system [33,45], our findings highlight the good performance of MMSNP-PNIPAM-co-MPS as a drug delivery system.

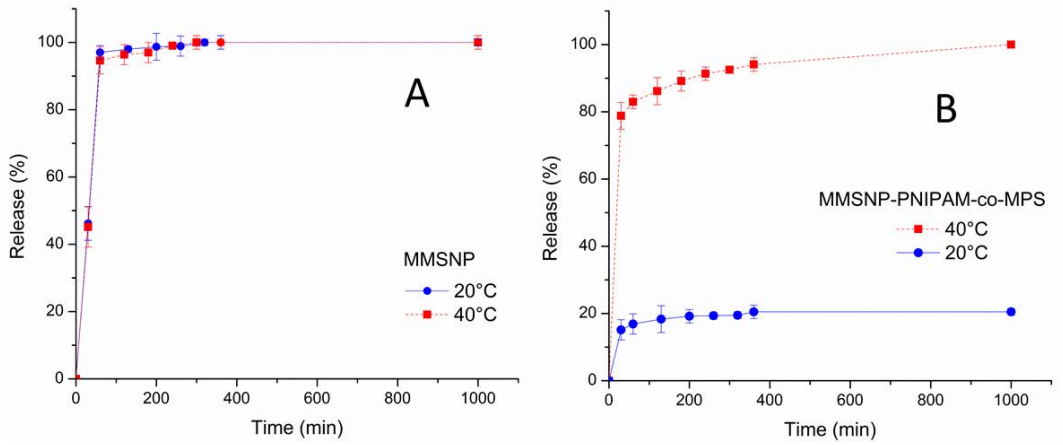

Fig. 9. Ibuprofen release curves by A) MMSNP and B) MMSNP-PNIPAM-co-MPS samples at 20 °C (blue circles and solid line) and 40°C (red squares and dotted line).

4. Conclusions

In this study, we have prepared hybrid thermoresponsive polymer-grafted magnetic mesoporous silica-based nanocarriers. A simple one-step procedure to graft the thermoresponsive copolymer PNIPAM-*co*-MPS on the particles was adopted. The hybrid nanoparticles have a typical size around 91 nm, a specific surface area of 505 $m^2 g^{-1}$ and a pore volume of 0.29 $cm^3 g^{-1}$. They present ferromagnetic properties with high magnetic saturation (19.5 emu g^{-1}), suggesting that they could be easily guided to a target site by an external magnetic field. The hybrid nanoparticles are monodisperse in aqueous medium and show a temperature dependence of the average hydrodynamic diameter, which encourage their use as drug nanocarriers. They showed excellent temperature-controlled on-off release of the model drug. In particular, low % release of ibuprofen below LCST and a complete and fast ibuprofen release above the LCST, compared to previous report, was obtained [47–50]. Hence, MMSNP-PNIPAM-co-MPS with thermal and magnetic response are promising candidates for targeted drug delivery applications.

Acknowledgments

This project has received funding from the European Union's Horizon 2020 research and innovative programme under the Marie Sklodowska-Curie grant agreement No 645551 and from Universidad Nacional del Comahue (Project 04/I217). M.E. Peralta thanks the CONICET for his research graduate grant. L. Carlos is a research member of CONICET (Argentina). D. Mártire is a research member of CIC (Buenos Aires, Argentina). Additionally, authors would like to thank Dr. Maria Carmen Valsania (University of Torino, Italy) for TEM measurements and Dr. Alejandro Butera for magnetic measurements (Centro Atómico Bariloche, Argentina).

Supporting Material

The supporting information file with TEM image of synthesized iron oxide nanoparticles, full range ATR-FTIR spectra of MMSNP-PNIPAM-co-MPS and MMSNP and table of magnetic properties of the nanocarriers is available.

References

[1] S. Mura, J. Nicolas, P. Couvreur, Stimuli-responsive nanocarriers for drug delivery, Nat.

Mater. 12 (2013) 991–1003. doi:10.1038/nmat3776.
[2] Z. Li, E. Ye, David, R. Lakshminarayanan, X.J. Loh, Recent Advances of Using Hybrid Nanocarriers in Remotely Controlled Therapeutic Delivery, Small. 12 (2016) 4782–4806. doi:10.1002/smll.201601129.
[3] J. Wen, K. Yang, F. Liu, H. Li, Y. Xu, S. Sun, Diverse gatekeepers for mesoporous silica nanoparticle based drug delivery systems, Chem. Soc. Rev. 46 (2017) 6024–6045. doi:10.1039/C7CS00219J.
[4] M. Vallet-Regi, A. Rámila, R.P. Del Real, J. Pérez-Pariente, A new property of MCM-41: Drug delivery system, Chem. Mater. 13 (2001) 308–311. doi:10.1021/cm0011559.
[5] F. Tang, L. Li, D. Chen, Mesoporous silica nanoparticles: Synthesis, biocompatibility and drug delivery, Adv. Mater. 24 (2012) 1504–1534. doi:10.1002/adma.201104763.
[6] Y. Yang, C. Yu, Advances in silica based nanoparticles for targeted cancer therapy, Nanomedicine Nanotechnology, Biol. Med. 12 (2016) 317–332. doi:10.1016/j.nano.2015.10.018.
[7] M.A. Agotegaray, V.L. Lassalle, Silica-coated Magnetic Nanoparticles An Insight into Targeted Drug Delivery and Toxicology, Springer Nature, Cham, Switzerland, 2017.
[8] Y. Tian, A. Glogowska, W. Zhong, T. Klonisch, M. Xing, Polymeric mesoporous silica nanoparticles as a pH-responsive switch to control doxorubicin intracellular delivery, J. Mater. Chem. B. 1 (2013) 5264. doi:10.1039/c3tb20544d.
[9] L. Xiong, J. Bi, Y. Tang, S.Z. Qiao, Magnetic Core-Shell Silica Nanoparticles with Large Radial Mesopores for siRNA Delivery, Small. 12 (2016) 4735–4742. doi:10.1002/smll.201600531.
[10] N. An, H. Lin, C. Yang, T. Zhang, R. Tong, Y. Chen, F. Qu, Gated magnetic mesoporous silica nanoparticles for intracellular enzyme-triggered drug delivery, Mater. Sci. Eng. C. 69 (2016) 292–300. doi:10.1016/j.msec.2016.06.086.
[11] Q. Zhao, S. Wang, Y. Yang, X. Li, D. Di, C. Zhang, T. Jiang, S. Wang, Hyaluronic acid and carbon dots-gated hollow mesoporous silica for redox and enzyme-triggered targeted drug delivery and bioimaging, Mater. Sci. Eng. C. 78 (2017) 475–484. doi:10.1016/J.MSEC.2017.04.059.
[12] H. Li, J.Z. Zhang, Q. Tang, M. Du, J. Hu, D. Yang, Reduction-responsive drug delivery based on mesoporous silica nanoparticle core with crosslinked poly(acrylic acid) shell, Mater. Sci. Eng. C. 33 (2013) 3426–3431. doi:10.1016/J.MSEC.2013.04.033.
[13] X. Chen, H. Sun, J. Hu, X. Han, H. Liu, Y. Hu, Transferrin gated mesoporous silica nanoparticles for redox-responsive and targeted drug delivery, Colloids Surfaces B Biointerfaces. 152 (2017) 77–84. doi:10.1016/J.COLSURFB.2017.01.010.
[14] K.L. Hamner, C.M. Alexander, K. Coopersmith, C. Provenza, D. Reishofer, M.M. Maye, Using Temperature Sensitive Smart Polymers to Regulate DNA-Mediated Nano Assembly and Encoded Nano Carrier Drug Release, ACS Nano. 7 (2013) 7011–7020. doi:10.1021/nn402214e.
[15] S.A. Jadhav, I. Miletto, V. Brunella, G. Berlier, D. Scalarone, Controlled post-synthesis grafting of thermoresponsive poly(*N* -isopropylacrylamide) on mesoporous silica nanoparticles, Polym. Adv. Technol. 26 (2015) 1070–1075. doi:10.1002/pat.3534.
[16] P. Saint-Cricq, S. Deshayes, J.I. Zink, A.M. Kasko, Magnetic field activated drug delivery using thermodegradable azo-functionalised PEG-coated core–shell mesoporous silica nanoparticles, Nanoscale. 7 (2015) 13168–13172. doi:10.1039/C5NR03777H.
[17] J. Paris, M. Cabañas, M. Manzano, M.V.-R.-A. Nano, U. 2015, Polymer-grafted mesoporous silica nanoparticles as ultrasound-responsive drug carriers, ACS Publ. 9 (2015) 11023–11033.
[18] N.K. Mal, M. Fujiwara, Y. Tanaka, Photocontrolled reversible release of guest molecules from coumarin- modified mesoporous silica, Nature. 421 (2003) 350–353. doi:10.1038/nature01337.1.
[19] F. Wang, A. Klaikherd, S. Thayumanavan, Temperature sensitivity trends and multi-

stimuli sensitive behavior in amphiphilic oligomers, J. Am. Chem. Soc. 133 (2011) 13496–13503. doi:10.1021/ja204121a.
[20] R. Liu, M. Fraylich, B.R. Saunders, Thermoresponsive copolymers: from fundamental studies to applications, Colloid Polym. Sci. 287 (2009) 627–643. doi:10.1007/s00396-009-2028-x.
[21] E. Guisasola, A. Baeza, M. Talelli, D. Arcos, M. Moros, J.M. de la Fuente, M. Vallet-Regí, Magnetic-Responsive Release Controlled by Hot Spot Effect, Langmuir. 31 (2015) 12777–12782. doi:10.1021/acs.langmuir.5b03470.
[22] R.R. Kokardekar, V.K. Shah, H.R. Mody, PNIPAM Poly (N-isopropylacrylamide): A Thermoresponsive "Smart" Polymer in Novel Drug Delivery System, Med. Updat. 7 (2012) 60–63.
[23] L.A. Picos-Corrales, A. Licea-Claverie, J.M. Cornejo-Bravo, S. Schwarz, K.F. Arndt, Well-defined N-isopropylacrylamide dual-sensitive copolymers with LCST ≈38 °c in different architectures: Linear, block and star polymers, Macromol. Chem. Phys. 213 (2012) 301–314. doi:10.1002/macp.201100468.
[24] V. Brunella, S.A. Jadhav, I. Miletto, G. Berlier, E. Ugazio, S. Sapino, D. Scalarone, Hybrid drug carriers with temperature-controlled on-off release: A simple and reliable synthesis of PNIPAM-functionalized mesoporous silica nanoparticles, React. Funct. Polym. 98 (2016) 31–37. doi:10.1016/j.reactfunctpolym.2015.11.006.
[25] E. Yu, A. Lo, L. Jiang, B. Petkus, N. Ileri Ercan, P. Stroeve, Improved controlled release of protein from expanded-pore mesoporous silica nanoparticles modified with co-functionalized poly(n-isopropylacrylamide) and poly(ethylene glycol) (PNIPAM-PEG), Colloids Surfaces B Biointerfaces. 149 (2017) 297–300. doi:10.1016/j.colsurfb.2016.10.033.
[26] E. Aznar, M. Oroval, L. Pascual, J.R. Murguía, R. Martínez-Máñez, F. Sancenón, Gated Materials for On-Command Release of Guest Molecules, Chem. Rev. 116 (2016) 561–718. doi:10.1021/acs.chemrev.5b00456.
[27] F. Zhang, G.B. Braun, A. Pallaoro, Y. Zhang, Y. Shi, D. Cui, M. Moskovits, D. Zhao, G.D. Stucky, Mesoporous multifunctional upconversion luminescent and magnetic "nanorattle" materials for targeted chemotherapy, Nano Lett. 12 (2011) 61–67. doi:10.1021/nl202949y.
[28] N.Ž. Knežević, E. Ruiz-Hernández, W.E. Hennink, M. Vallet-Regí, Magnetic mesoporous silica-based core/shell nanoparticles for biomedical applications, RSC Adv. 3 (2013) 9584. doi:10.1039/c3ra23127e.
[29] J. Kim, H.S. Kim, N. Lee, T. Kim, H. Kim, T. Yu, I.C. Song, W.K. Moon, T. Hyeon, Multifunctional uniform nanoparticles composed of a magnetite nanocrystal core and a mesoporous silica shell for magnetic resonance and fluorescence imaging and for drug delivery, Angew. Chemie - Int. Ed. 47 (2008) 8438–8441. doi:10.1002/anie.200802469.
[30] S. Xuan, F. Wang, J.M.Y. Lai, K.W.Y. Sham, Y.J. Wang, S. Lee, J.C. Yu, C.H.K. Cheng, K.C. Leung, Synthesis of Biocompatible , Mesoporous Fe 3 O 4 Nano / Microspheres with Large Surface Area for Magnetic Resonance Imaging and Therapeutic Applications, Interfaces (Providence). (2011) 237–244. doi:10.1039/c1jm13357h.
[31] B. Sahoo, K.S.P. Devi, S. Dutta, T.K. Maiti, P. Pramanik, D. Dhara, Biocompatible mesoporous silica-coated superparamagnetic manganese ferrite nanoparticles for targeted drug delivery and MR imaging applications, J. Colloid Interface Sci. 431 (2014) 31–41. doi:10.1016/j.jcis.2014.06.003.
[32] Y. Chen, K. Ai, J. Liu, G. Sun, Q. Yin, L. Lu, Multifunctional envelope-type mesoporous silica nanoparticles for pH-responsive drug delivery and magnetic resonance imaging, Biomaterials. 60 (2015) 111–120. doi:10.1016/j.biomaterials.2015.05.003.
[33] M. Hegazy, P. Zhou, G. Wu, L. Wang, N. Rahoui, N. Taloub, X. Huang, Y. Huang, Construction of polymer coated core–shell magnetic mesoporous silica nanoparticles with triple responsive drug delivery, Polym. Chem. (2017) 5852–5864.

doi:10.1039/C7PY01179B.
[34] Z. Tian, X. Yu, Z. Ruan, M. Zhu, Y. Zhu, N. Hanagata, Magnetic mesoporous silica nanoparticles coated with thermo-responsive copolymer for potential chemo- and magnetic hyperthermia therapy, Microporous Mesoporous Mater. 256 (2018) 1–9. doi:10.1016/j.micromeso.2017.07.053.
[35] Y. Deng, D. Qi, C. Deng, X. Zhang, D. Zhao, Superparamagnetic High-Magnetization Microspheres with an Fe3O4@SiO2 Core and Perpendicularly Aligned Mesoporous SiO2 Shell for Removal of Microcystins, J. Am. Chem. Soc. 130 (2008) 28–29. doi:10.1016/j.colsurfa.2012.03.019.
[36] I. Miletto, E. Bottinelli, G. Caputo, S. Coluccia, E. Gianotti, Bright photoluminescent hybrid mesostructured silica nanoparticles, Phys. Chem. Chem. Phys. 14 (2012) 10015. doi:10.1039/c2cp40975e.
[37] G. Berlier, L. Gastaldi, E. Ugazio, I. Miletto, P. Iliade, S. Sapino, Stabilization of quercetin flavonoid in MCM-41 mesoporous silica: positive effect of surface functionalization, J. Colloid Interface Sci. 393 (2013) 109–118. doi:10.1016/J.JCIS.2012.10.073.
[38] S.A. Jadhav, V. Brunella, D. Scalarone, G. Berlier, Poly(NIPAM-co-MPS)-grafted multimodal porous silica nanoparticles as reverse thermoresponsive drug delivery system, Asian J. Pharm. Sci. 12 (2017) 279–284. doi:10.1016/j.ajps.2017.02.002.
[39] E.C. Sklute, S. Kashyap, M.D. Dyar, J.F. Holden, T. Tague, P. Wang, S.J. Jaret, Spectral and morphological characteristics of synthetic nanophase iron (oxyhydr)oxides, Phys. Chem. Miner. 45 (2018) 1–26. doi:10.1007/s00269-017-0897-y.
[40] F.B. Zanardi, I.A. Barbosa, P.C. De Sousa Filho, L.D. Zanatta, D.L. Da Silva, O.A. Serra, Y. Iamamoto, Manganese porphyrin functionalized on Fe3O4@nSiO2@MCM-41 magnetic composite: Structural characterization and catalytic activity as cytochrome P450 model, Microporous Mesoporous Mater. 219 (2016) 161–171. doi:10.1016/j.micromeso.2015.07.035.
[41] E. Bittrich, S. Burkert, M. Müller, K.-J. Eichhorn, M. Stamm, P. Uhlmann, Temperature-Sensitive Swelling of Poly(N-isopropylacrylamide) Brushes with Low Molecular Weight and Grafting Density, Langmuir. 28 (2012) 3439–3448. doi:10.1021/la204230a.
[42] M. Thommes, K. Kaneko, A. V. Neimark, J.P. Olivier, F. Rodriguez-Reinoso, J. Rouquerol, K.S.W. Sing, Physisorption of gases, with special reference to the evaluation of surface area and pore size distribution (IUPAC Technical Report), Pure Appl. Chem. 87 (2015) 1051–1069. doi:10.1515/pac-2014-1117.
[43] S.A. Jadhav, V. Brunella, I. Miletto, G. Berlier, D. Scalarone, Synthesis of poly(N-isopropylacrylamide) by distillation precipitation polymerization and quantitative grafting on mesoporous silica, J. Appl. Polym. Sci. 133 (2016) 1–8. doi:10.1002/app.44181.
[44] X. Hou, H. Xu, L. Pan, Y. Tian, X. Zhang, L. Ma, Y. Li, J. Zhao, Adsorption of bovine serum albumin on superparamagnetic composite microspheres with a Fe_3O_4/SiO_2 core and mesoporous SiO_2 shell, RSC Adv. 5 (2015) 103760–103766. doi:10.1039/C5RA21773C.
[45] L. Dong, H. Peng, S. Wang, Z. Zhang, J. Li, F. Ai, Q. Zhao, M. Luo, H. Xiong, L. Chen, Thermally and magnetically dual-responsive mesoporous silica nanospheres: Preparation, characterization, and properties for the controlled release of sophoridine, J. Appl. Polym. Sci. 131 (2014). doi:10.1002/app.40477.
[46] B.-S. Tian, C. Yang, Thermo-Sensitive Poly(N-Isopropylacrylamide)/Mesoporous Silica Nanocomposites as Controlled Delivery Carriers: Loading and Release Behaviors for Drug Ibuprofen, J. Nanosci. Nanotechnol. 11 (2011) 1871–1879. doi:10.1166/jnn.2011.3543.
[47] X. Jin, Q. Wang, J. Sun, H. Panezail, X. Wu, S. Bai, Dual temperature- and pH-responsive ibuprofen delivery from poly(N-isopropylacrylamide-co-acrylic acid) nanoparticles and their fractal features, Polym. Bull. 74 (2017) 3619–3638. doi:10.1007/s00289-017-1915-4.

[48] M. Bathfield, J. Reboul, T. Cacciaguerra, P. Lacroix-Desmazes, C. Gérardin, Thermosensitive and Drug-Loaded Ordered Mesoporous Silica: A Direct and Effective Synthesis Using PEO-b-PNIPAM Block Copolymers, Chem. Mater. 28 (2016) 3374–3384. doi:10.1021/acs.chemmater.6b00595.

[49] S. Zhu, C. Chen, Z. Chen, X. Liu, Y. Li, Y. Shi, D. Zhang, Thermo-responsive polymer-functionalized mesoporous carbon for controlled drug release, Mater. Chem. Phys. 126 (2011) 357–363. doi:10.1016/j.matchemphys.2010.11.013.

[50] Y.Z. You, K.K. Kalebaila, S.L. Brock, D. Oupický, Temperature-controlled uptake and release in PNIPAM-modified porous silica nanoparticles, Chem. Mater. 20 (2008) 3354–3359. doi:10.1021/cm703363w.